Journal of Plankton Research Vol.16 no.9 pp.1167–1196, 1994

Growth and phosphorus uptake of summer phytoplankton in Lake Erken (Sweden)

Vera Istvánovics, Judit Padisák, Kurt Pettersson[1] and Donald C.Pierson[2]

Balaton Limnological Research Institute, H-8237 Tihany, Hungary, [1]Erken Laboratory, Institute of Limnology, Uppsala University, Norr Malma 4200, S-76173 Norrtälje, Sweden and [2]Ben Nesin Laboratory, Rt28A, Shokan, NY 12481, USA

Abstract. The thermal stratification in Lake Erken was short and relatively unstable in 1989. Changes in the species composition of the phytoplankton between early May and August followed the general succession pattern outlined for other temperate lakes. Fast-growing, r-strategist cryptophytes, dominant in the early phase of succession, could be separated sufficiently by 12 μm membrane filters from larger K-strategists like *Ceratium hirundinella* and *Gloeotrichia echinulata* which dominated in July. Under more turbulent conditions, the biomass of diatoms increased, and these species were also >12 μm. Growth rates of the phytoplankton and those of the two size groups were sensitive to the species composition, but fitted reasonably to the Droop model. Long turnover times of orthophosphate in the water, the Phosphorus Deficiency Indicator defined here as the ratio of the light-saturated rate of photosynthesis and the conductivity coefficient of phosphate uptake, and relative growth rates generally indicated low P-deficiency. Moderate deficiency was observed in late July, towards the end of the stratification period. Steady-state net P-uptake rates were calculated from the Droop model and compared with instantaneous net P-uptake rates estimated from ^{32}P uptake kinetics by the linear force–flow relationship of Falkner et al. (*Arch. Microbiol.*, **152**, 353–361, 1989). The two data sets showed surprisingly similar seasonal trends. Depletion of epilimnetic soluble reactive phosphorus (SRP) resulted in enhanced utilization of intracellularly stored P. Such periods were, however, interrupted by elevated SRP inputs to the epilimnion that led to luxury P uptake and a low incidence of P deficiency.

Introduction

The species composition of the phytoplankton is controlled by a set of hierarchically structured physical, chemical and biological variables. The master variables are physical factors which influence chemical and biological factors in different ways. When the physical conditions are relatively stable, like for example during the summer stratification, the main selective variables are shaped by the activities of the planktonic organisms, and this gives rise to true autogenic succession (Reynolds, 1988, 1989; Sommer, 1989a). In the early phase of succession, when both stress and disturbance are low, fast-growing, r-selected species will be present. Later, when disturbance is still low but increasing stress sharpens interspecific competition, K-selected, loss-resistant species become dominant.

Partitioning of resource gradients by two co-existing species has long been established by mathematical models and in chemostat experiments (Tilman and Kilham, 1976; Tilman, 1977; Tilman *et al.*, 1982). Competitive co-existence of several species is possible when the nutrient supplies are pulsed (Sommer, 1984). Under such conditions, an oscillating equilibrium is established, in which the biomass of storage-specialist (low maximum growth rate, μ_m, relative to maximum phosphate uptake velocity, u_m) and affinity-adapted (high μ_m/K_s)

algae remains constant, whereas the biomass of velocity-adapted species (high μ_m, high u_m) follows the nutrient pulses.

The models of Monod (1950) and Droop (1973) have often been shown to adequately describe *in situ* growth of the phytoplankton (Olsen *et al.*, 1983; Auer *et al.*, 1986; Vadstein *et al.*, 1988; Sommer, 1989b). According to the Monod model, specific growth rates (μ, day^{-1}) are a hyperbolic function of the external phosphate concentration ($[P_e]$, $\mu g\ P\ l^{-1}$):

$$\mu = \mu_m \times \frac{[P_e]}{(K_s + [P_e])} \tag{1}$$

where μ_m (day^{-1}) is the maximum specific growth rate at infinite external substrate concentration and K_s ($\mu g\ P\ l^{-1}$) is the half-saturation constant of growth with respect to phosphorus.

Microorganisms, however, may store the limiting nutrient before they convert it into new biomass with a certain efficiency. Algal growth is frequently based on the internal P stores (Fitzgerald and Nelson, 1966; Droop, 1973). Droop (1973) related specific growth rates to the phosphorus cell quota (Q_P, $\mu g\ P\ mg^{-1}\ C$):

$$\mu = \mu'_m \times \left(1 - \frac{Q_{P,0}}{Q_P}\right) \tag{2}$$

where μ'_m (day^{-1}) is the maximum specific growth rate at infinite internal substrate concentration and $Q_{P,0}$ ($\mu g\ P\ mg^{-1}\ C$) is the maintenance cell quota.

P-uptake by algae in relation to their growth and cell quotas has been studied intensely both in monospecific (Rhee, 1973; Tilman and Kilham, 1976; Nalewajko and Lean, 1978) and multispecific chemostats (Smith and Kalff, 1983; Vadstein and Olsen, 1989). Under steady-state, balanced-growth conditions, the specific net phosphate uptake rate (u_P, $\mu g\ P\ mg^{-1}\ C\ h^{-1}$) is proportional to the growth rate (Droop, 1973):

$$u_P = \mu \times Q_P \tag{3}$$

At the same time, the relationship between P uptake and growth has remained poorly understood under *in situ* conditions, primarily due to a lack of appropriate methods to obtain net phosphate uptake rates at low P concentrations prevailing in P-deficient lakes. The most widely applied isotopic method yields uptake rate constants which must be multiplied by the phosphate concentration in order to get uptake rates. The real orthophosphate concentration is overestimated by the chemical analysis (Rigler, 1966) and often falls below the detection limit. Moreover, the isotopically determined uptake rate constant is a gross value, the sum of the net uptake and leakage rate constants (Lean and Nalewajko, 1976; Nalewajko and Lean, 1978; Lean and White, 1983; Istvánovics and Herodek, 1995).

Recently, Falkner *et al.* (1989) have presented a conceptual phosphate uptake model, the background of which is that P uptake reflects, in kinetic and

energetic terms, the conversion of external phosphate to polyphosphates. The lower the external phosphate concentration, the more energy must be used in polyphosphate formation. Net uptake ceases at a threshold concentration, $[P_e]_T$, since the available energy is then insufficient to support polyphosphate formation. This model has the simple form:

$$v_{net} = L_P \times (\log[P_e] - \log[P_e]_T) \quad (4)$$

where v_{net} (μg P mg^{-1} C h^{-1}) is the specific transient-state net phosphate uptake rate and L_P (μg P mg^{-1} C h^{-1}) is the conductivity coefficient which reflects the activity of the phosphate carrier in the cell membrane.

Based on the force–flow relationship and with the assumptions that (i) the leakage rate is a physiologically dependent constant at any external phosphate concentrations and (ii) pure leakage rates can be estimated in water samples without P addition, it was possible to simultaneously estimate net P uptake and leakage rates from ^{32}P uptake data (Istvánovics and Herodek, 1995).

In the present study, we followed changes in the species composition of phytoplankton in Lake Erken from early May until early August. Growth and phosphorus uptake of the phytoplankton community, and those of two different algal size groups (3–12 and >12 μm), were measured in order to assess possible interspecific differences in growth and P uptake strategies.

Method

Lake Erken is a moderately eutrophic lake in southern Sweden with a surface area of 24 km^2 and a mean depth of 9 m. Summer stratification usually lasts from early June until early September. During this period, the external phosphorus loading is <0.02 mg P m^{-2} day^{-1} (Pettersson, 1985).

In 1989, water samples were taken weekly between 8 May and 8 August with an electric pump at a buoy situated 700 m offshore, above the deepest point of the lake (Z_{max} = 21 m). The water was sampled between 8:00 and 8:30 in the morning at different depths, and transported in non-transparent 2 l bottles to the near-shore laboratory. In this paper, we rely mostly on data obtained at 3 m depth.

Underwater photosynthetically active radiation (PAR; 400–700 nm) profiles were determined with a Li-Cor light meter during sampling. Water temperature was measured automatically at 16–25 depths at 1 min intervals using thermocouple sensors of 0.05°C resolution. Mean temperature profiles were saved at 30 min intervals. The mixing depth (Z_m) was estimated from 1°C isotherm plots calculated from the automated temperature records (Pierson *et al.*, 1992).

Soluble reactive phosphorus (SRP) was determined as molybdate-reactive P (Murphy and Riley, 1962). Surplus P (SP) was measured according to Fitzgerald and Nelson (1966) with minor modifications (Pettersson, 1980). Particulate P (PP) and total P (TP) were measured after persulfate oxidation (Menzel and Corvin, 1965). PP and SP were fractionated by filtering the samples onto 0.2, 3 and 12 μm cellulose acetate membrane filters (Schleicher and Schüll).

Ammonia, nitrite and nitrate were measured according to standard methods (Ahlgren and Ahlgren, 1976).

In order to determine chlorophyll *a* and particulate carbon (PC), lake water and filtrates of 3 and 12 μm membrane filters were filtered onto Whatman GF/F glass fiber filters. Chlorophyll *a* samples were immediately transferred into 9 ml of 90% acetone and kept in the dark at 4°C for 24–36 h. Chlorophyll *a* was determined fluorometrically and corrected for degradation products according to Strickland and Parsons (1972). PC was measured with a CHN analyser on pre-combusted Whatman GF/F glass fiber filters (Carlo-Erba).

Phytoplankton in the unfiltered samples and in the filtrates of 3 and 12 μm membrane filters were fixed with acid Lugol's solution, and counted under an inverted microscope. The counting error was 10% (95% confidence limits; Lund *et al.*, 1958). Volumes of the species were taken from Nauwerck's (1963) data obtained in Lake Erken, with the exception of *Gloeotrichia echinulata*. Dimensions of single filaments, filament fragments and cells of this species were measured, and a colony was assumed to consist of 100 filaments. Biomass was estimated from cell numbers and specific volumes. Surfaces of the individual species were calculated according to Dokulil (1979) and Németh and Vörös (1986). The carbon content of the phytoplankton was estimated from the allometric relationship of Rocha and Duncan (1985). A higher conversion factor was used for *Rhodomonas* spp. (Vadstein *et al.*, 1988; Table I).

Net rates of biomass changes of the dominant species, positive (k^+, day^{-1}) or negative (k^-, day^{-1}), were calculated from the growth equation, $\ln N_t = \ln N_0 + k \times t$, where N is the number of cells and t is time in days.

Light-saturated rates of photosynthesis (P_m, μg C l^{-1} h^{-1}) were determined using a small volume–short term (5 ml–20 min) incubation method as described by Pierson (1990). The percentage distribution of the incorporated ^{14}C between different size groups was determined by measuring radioactivities retained on 0.2, 3 and 12 μm membrane filters after a 2 h incubation.

Growth rates (μ^*, day^{-1}) were estimated from the equation, $\mu = \ln(P_m/B)$, where B is the biomass expressed as cell carbon (μg C l^{-1}). P_m was multiplied by the number of daylight hours minus two. When the mixing depth exceeded the depth of the euphotic zone, the daily production rate was decreased proportionately to this ratio.

Phosphate uptake kinetics was determined in triplicate samples at zero-added P and in duplicates at different P additions (0.5, 1.0, 2.0 and 4.0 μg P l^{-1}) with carrier-free $H_3{}^{32}PO_4$ as described by Istvánovics *et al.* (1992). Partitioning of P uptake between different size groups was measured in the filtrates of 0.2, 3 and 12 μm membrane filters. Uptake rate constants were calculated as slopes of the linear regression lines of ln-transformed radioactivities plotted against time (Rigler, 1966).

P-uptake data were analyzed by the linear force–flow model of Falkner *et al.* (1989). The initial orthophosphate concentration, as well as the net and gross P-uptake rates, were estimated by an iterative procedure (Istvánovics and Herodek, 1995). According to this approach, leakage can be viewed as an

Table I. Characteristics of the dominant algal species in Lake Erken

Species/group	V (μm^3)	A/V (μm^{-1})	C^*/V (pg C μm^{-3})	$C^*/chl\ a$ (μg C μg^{-1} chl a)	L_P/A (fg P μm^{-1} h^{-1})	$[P_e]_T$ (μg P l^{-1})
Rhodomonas	100	0.90	0.280	50–60	0.108 ± 0.081	0.42 ± 0.31
					0.018 ± 0.198	0.10 ± 0.91
Cryptomonas	2500	0.45	0.264	50–180	0.068 ± 0.050	0.54 ± 0.32
					0.015 ± 0.115	0.17–0.73
Anabaena circinalis	150	0.90	0.268	–	–	–
Gloeotrichia echinulata	9500	0.74	0.140	30–300	–	>20[a]
Ceratium hirundinella	75 000	0.15	0.136	300	0.480	0.30
Asterionella, Fragilaria	800	0.68	0.113	190	0.190 ± 0.067	0.51 ± 0.18
					0.139 ± 0.166	0.35–0.70
Stephanodiscus, Cyclotella	2500	0.27	0.113	–	0.241 ± 0.154	1.01 ± 0.84
					0.072 ± 0.376	0.35–1.96

V = volume; A = surface; C^* = estimated cell carbon; L_P = conductivity coefficient; $[P_e]_T$ = threshold concentration.
[a] From Istvánovics *et al.* (1993).

apparent P uptake which shifts the true $[P_e]_T$ threshold value to an apparent $[P'_e]_T$ value (Figure 1):

$$v_{gross} = v_{net} + v_{leak} = k_{gross} \times ([P_a] + [P_e]_0) = L_P \times \{\log([P_a] + [P_e]_0) - \log[P_e]_T\} + v_{leak} = L_P \times \{\log([P_a] + [P_e]_0) - \log[P'_e]_T\} \quad (5)$$

where v_{gross} (μg P mg^{-1} C h^{-1}) is the specific gross phosphate uptake rate, v_{leak} (μg P mg^{-1} C h^{-1}) is the specific phosphate leakage rate, k_{gross} (mg^{-1} C h^{-1}) is the specific gross uptake rate constant, $[P_a]$ (μg P l^{-1}) is the added phosphate concentration and $[P_e]_0$ (μg P l^{-1}) is the initial phosphate concentration.

Community P-uptake rate is the sum of the uptake rates of the individual species, so that community average P uptake follows the simple force–flow relationship until the external concentration falls to the threshold of the species present with the highest threshold (Figure 1). Net uptake by the community ceases when the threshold of the species with the minimum threshold has been reached. At this latter $[P_e]_0$ concentration, the isotopic method yields an estimate of the leakage rate constant, k_{leak}, and the rate of leakage is:

$$v_{leak} = k_{leak} \times [P_e]_0 = L_P \times (\log[P_e]_T - \log[P'_e]_T) \quad (6)$$

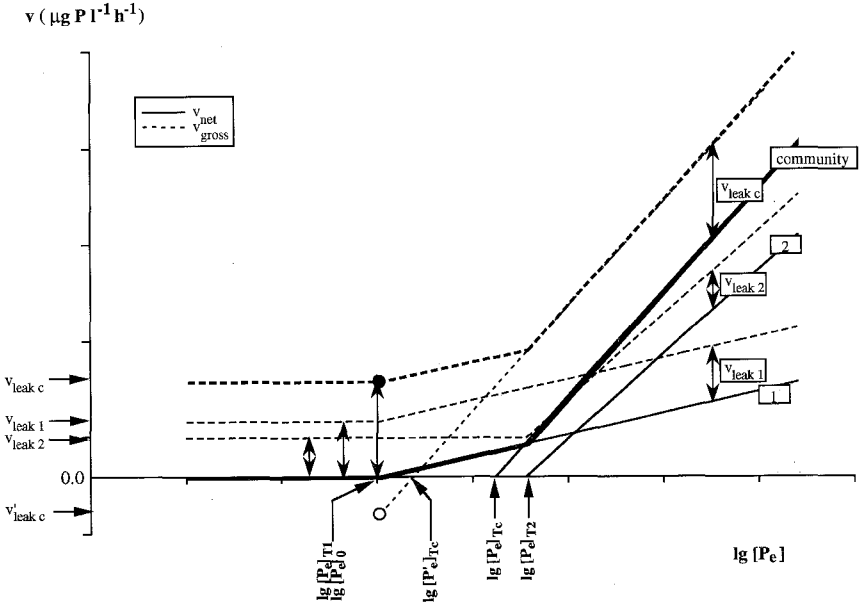

Fig. 1. Thellier plot of the P-uptake model of Falkner *et al.* (1989) indicating net and gross P uptake rate (v) curves of a two-species 'community'. v_{leak} = leakage rate, v'_{leak} = leakage rate predicted by the community gross uptake curve, $[P_e]$ = external phosphate concentration, $[P_e]_T$ = threshold concentration, $[P'_e]_T$ = apparent threshold concentration, $[P_e]_0$ = initial phosphate concentration. Indexes 1, 2, c refer to species 1, species 2 and the community. Open symbol = v'_{leak} at $[P_e]_0$; closed symbol = v_{leak} measured at $[P_e]_0$.

However, the average gross P-uptake curve of the community has been obtained in a concentration range where all species contributed to net uptake, and therefore this curve predicts a lower than measured leakage rate, v'_{leak} (Figure 1).

$$v'_{leak} = k'_{leak} \times [P_e]_0 = L_P \times (\log[P_e]_0 - \log[P'_e]_T) \quad (7)$$

Substitution of these relationships into equation (5) results, after rearrangement, in:

$$k_{gross} \times [P_a] = L_P \times \log[P_a] - L_P \times \log[P_e]_0 + k'_{leak} \times [P_e]_0 + L_p \times \log(1 + [P_e]_0/[P_a]) - k_{gross} \times [P_e]_0 \quad (8)$$

Equation (8) can be used to approximate net and gross P-uptake rates of the plankton. In the first step, an approximate ${}^1v_{gross} = k_{gross} \times [P_a]$ value can be plotted against $\log[P_a]$. The slope of the linear regression line gives an approximate ${}^1L_P$ conductivity coefficient, and the intercept at the ordinate (${}^1a$) is:

$${}^1a = {}^1k'_{leak} \times {}^1[P_e]_0 - L_P \times \log{}^1[P_e]_0 \quad (9)$$

Equation (9) must be solved before continuing the iteration. The $y = f({}^1[P_e]_0) = {}^1a + {}^1L_P \times \log{}^1[P_e]_0 - {}^1k'_{leak} \times {}^1[P_e]_0$ is a continuous function with one maximum at $\partial f({}^1[P_e]_0)/\partial({}^1[P_e]_0) = 0$. Derivation results in:

$${}^1L_P \times 1/\ln 10 \times 1{}^1[P_e]_0 - {}^1k'_{leak} = 0 \quad (10)$$

There is a single (${}^1k'_{leak}$; ${}^1[P_e]_0$) data pair, which fulfills both equations (9) and (10), i.e. where equation (9) has only one root. This ${}^1[P_e]_0$ value can be found by replacing ${}^1k'_{leak}$ from equation (9) into equation (8):

$$\log{}^1[P_e]_0 = 1/\ln 10 - {}^1a/{}^1L_P \quad (11)$$

In the second step, a ${}^2v_{gross} = k_{gross} \times [P_a] - {}^1L_P \times \log(1 + {}^1[P_e]_0/[P_a]) + k_{gross} \times {}^1[P_e]_0$ value can be plotted against $\log[P_a]$. With the resulting (${}^2L_P$; ${}^2a$) data pair, equation (9) yields another (${}^2k'_{leak}$; ${}^2[P_e]_0$) value. The iteration is convergent.

Once the initial orthophosphate concentration, $[P_e]_0$, has been estimated, the rate of leakage can be calculated as $v_{leak} = k_{leak} \times [P_e]_0$. The gross uptake rate, $v_{gross} = k_{gross} \times ([P_a] + [P_e]_0)$ minus v_{leak}, gives the rate of net P uptake (Figure 1).

Results

Epilimnetic conditions

The water column started to stratify in mid-May and a sharp thermal gradient

had developed at 7 m by 29 May (Figure 2). However, the stratification was intermittent and the continuous summer stratification (>1°C m^{-1} temperature gradient) was not established until 22 June. Owing to the late onset of the stratification, the hypolimnion warmed up to >13°C. The stratification was unstable and short lasting (44 days), with a mean metalimnetic temperature gradient of 1.14°C m^{-1}. The depth of the epilimnion increased gradually from ~7 to 12 m and the average was 9.6 m.

The depth of the euphotic zone (Z_{eu}, 1% of PAR) varied between 5.7 and 9.7 m, whereas the mixing depth (Z_m) was 4–12 m. Z_{eu} exceeded or nearly

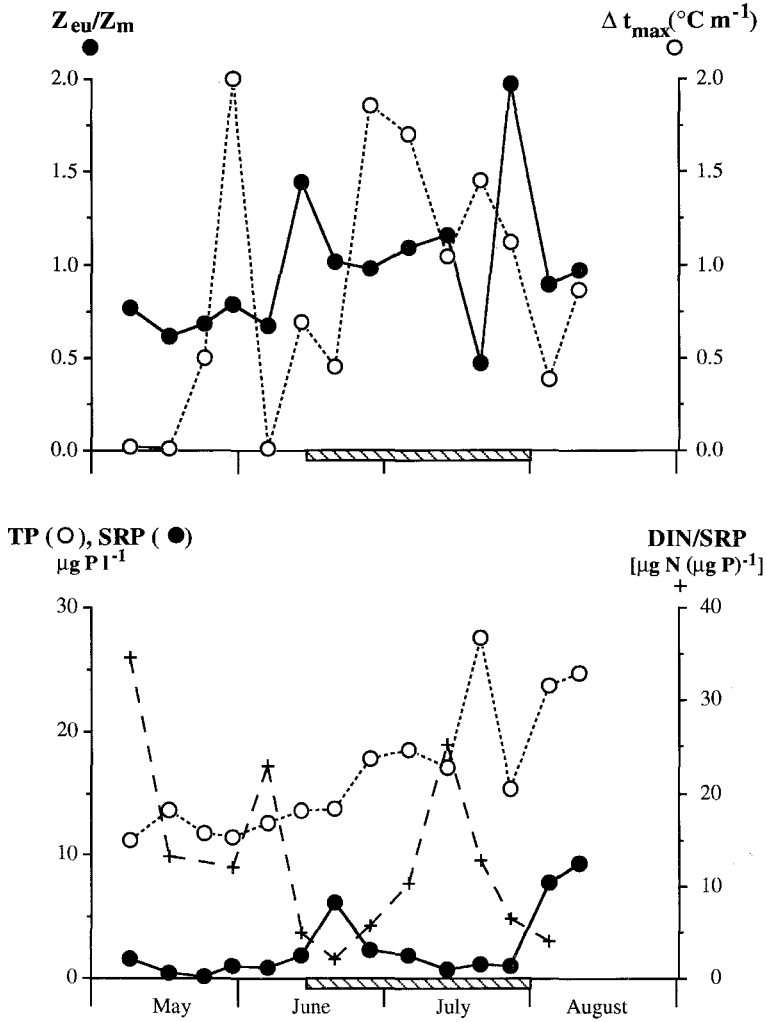

Fig. 2. Epilimnetic conditions during the study period. **Upper panel**: The ratios of the euphotic depth to the mixing depth (Z_{eu}/Z_m), and the maximum vertical temperature gradient (Δt_{max}). **Lower panel**: Concentrations of total P (TP) and soluble reactive P (SRP), and the ratio of dissolved inorganic nitrogen (DIN) to SRP at 3 m. (The period of permanent thermal stratification is shown on the horizontal axis.)

equaled Z_m during most of the thermal stratification. The minimum Z_{eu}/Z_m ratio of 0.47 coincided with the biomass maximum of *G.echinulata* (Figures 2 and 3).

Total-P concentration increased progressively (1.4% day^{-1}) in the epilimnion. Net total P loading from the sediments/hypolimnion could be estimated as 3 mg P m^{-2} day^{-1} in June–July (Figure 2). The SRP concentration peaked at 6.2 μg P l^{-1} on 19 June due to total mixing, since by this time a high SRP concentration had been established in the hypolimnion (Pettersson *et al.*, 1990, 1993; Pierson *et al.*, 1992). Elevated SRP concentrations were measured again in the epilimnion after the breakdown of the thermal stratification in early August.

The epilimnetic concentration of dissolved inorganic nitrogen (DIN = NO_3^- + NO_2^- + NH_4^+) was relatively stable during the stratified period (7–18 μg N l^{-1}, mean 11.3 ± 3.9). Higher values (22–32 μg N l^{-1}) were measured during complete mixing. The variation of the DIN/SRP ratios between 2 and 35 by weight was largely a result of varying SRP concentrations (Figure 2).

Species composition of phytoplankton

Our study started in early May, when the spring diatom bloom was collapsing (Figure 3). Diatoms (*Asterionella formosa* and *Stephanodiscus* spp.) were still dominant, but their biomass decreased by ~3% day^{-1} until early July.

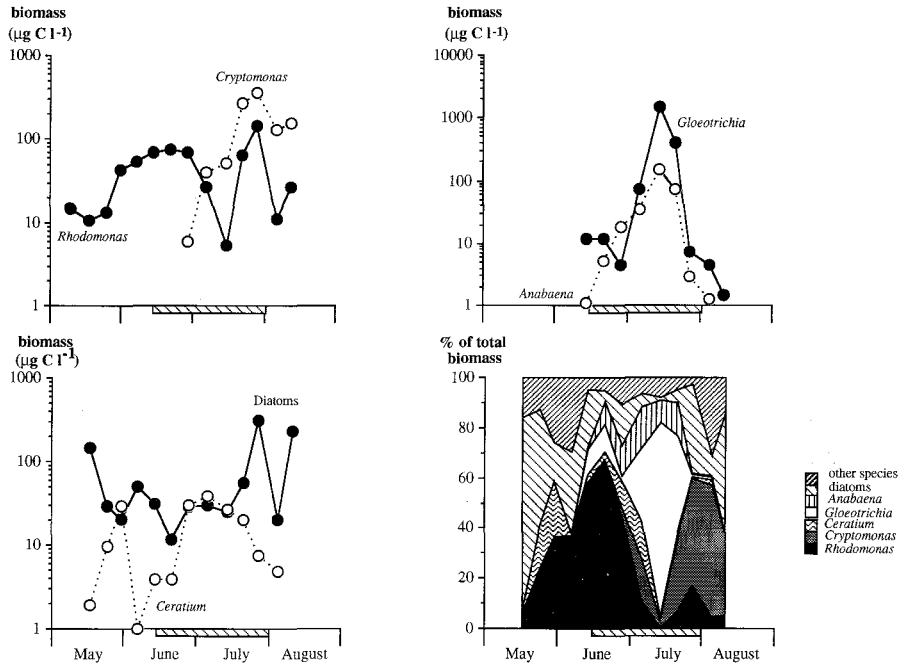

Fig. 3. Biomass of the dominant algal species and the species composition of the phytoplankton. (Biomass is expressed as estimated cell carbon. The period of permanent thermal stratification is shown on the horizontal axis.)

During May and June, small, fast-growing *Rhodomonas* spp. (primarily *Rhodomonas minuta* var. *nannoplanctonica*) were dominant, their carbon content made up 48–64% of total algal carbon in June. A steady-state population persisted for a month, showing little sensitivity to changes in nutrient or stability conditions (Figures 2 and 3).

When SRP was depleted, large, slow-growing species, first *Ceratium hirundinella*, thereafter *Anabaena circinalis* and *G.echinulata*, became dominant. *Ceratium hirundinella* maintained a steady-state population of 35 μg C l^{-1} for 3 weeks. The bloom of the latter two N_2-fixing cyanobacteria coincided with the minimum DIN/SRP ratios (<6 μg N μg^{-1} P; Figures 2 and 3).

In late July, the water column stability decreased, and the cyanobacterial bloom collapsed. Cryptophytes (*Cryptomonas* and *Rhodomonas* spp.) and different diatom species (*Asterionella formosa*, *Fragilaria* spp., *Cyclotella comta*, *Stephanodiscus* spp.) became dominant again (Figure 3). *Cryptomonas* spp. shared 40–70% of total algal carbon.

Total biomass (as carbon) of all the species not listed above remained, on average, <5 ± 2% during most of the study period. Elevated values (12–16%) were observed in early May and in early August during complete mixing, when varying diatom species were abundant for short periods.

In general, net rates of biomass changes of the dominant species (k^+ and k^-, day^{-1}) were similar to the corresponding values from Lake Constance (Sommer, 1981; Table II).

Estimates of algal biomass

In this study, 3 and 12 μm membrane filters were used to separate different size groups of plankton. Until mid-June, ~7% of the total bacterial production was associated with the >3 μm size fraction. Higher values (10–19%) were measured in late June and during July, when the proportion of attached to free-living bacteria probably increased.

Table II. Net rates of biomass changes of the dominant algal species (k^+ and k^-) in lakes Erken and Constance

Species/group	Lake Erken[a]		Lake Constance[b]	
	k^+ (day^{-1})	k^- (day^{-1})	k^+ (day^{-1})	k^- (day^{-1})
Rhodomonas	0.29 (2)	0.16 (2)	0.46–0.62	0.50–0.58
	0.37 (2)	0.31 (2)		
Cryptomonas	0.14 (5)	0.18 (2)	0.46–0.89	0.39–0.43
Anabaena circinalis	0.18 (4)	0.24 (4)	0.21–0.41	0.27–0.45
Gloeotrichia echinulata	0.32 (3)	0.38 (3)	–	–
Ceratium hirundinella	0.19 (3)	0.48 (2)	0.17	0.17
	0.15 (4)	0.10 (3)		
Asterionella, Fragilaria	0.30 (4)	0.16 (4)	0.27–0.36	0.25–0.40
Stephanodiscus, Cyclotella	0.06 (4)	0.13 (4)	0.10	0.10

Numbers in parentheses indicate the number of data points used to calculate net growth rates.
[a]Present study.
[b]Sommer (1981).

Separation of the dominant algal species by 12 μm membrane filters was fairly good. *Asterionella formosa*, *Stephanodiscus astraea*, *Fragilaria* spp., *C.comta* and *C.hirundinella* never passed this filter. Of the total biomass of *A.circinalis* and *G.echinulata*, 90–100% was >12 μm. *Rhodomonas* spp. always passed the 12 μm filter, and 80–100% of the *Cryptomonas* spp. cells were also found in the 3–12 μm size group. These two species made up 70–97% (mean 86.6 ± 9.2%) of the total biomass of the 3–12 μm fraction, except on 12 July when single filaments of *G.echinulata* reached 40% of the fractional biomass (as carbon). Only a negligible number of algal cells was observed in the filtrates of 3 μm membrane filters.

Even though separation of bacteria/algae and the dominant algal species was not complete, it was good enough to relate size-fractionated chemical data to the dominant algal species/assemblages present.

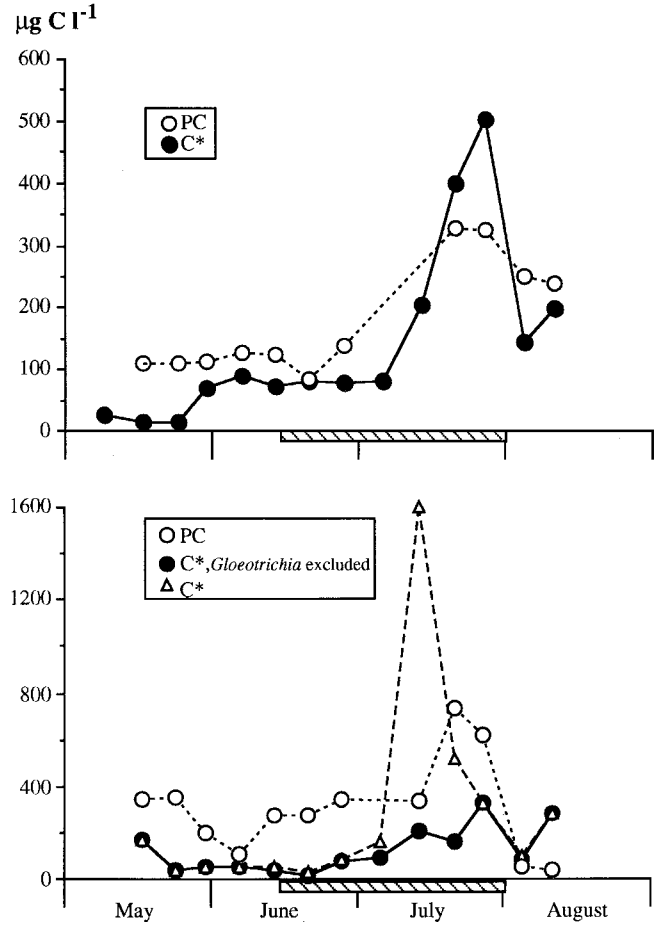

Fig. 4. Measured particulate carbon (PC), and carbon estimated from cell counts and volumes (C*). **Upper panel**: 3–12 μm algae; **lower panel**: >12 μm algae. (The period of permanent thermal stratification is shown on the horizontal axis.)

The relationship between carbon estimated from cell counts (C*) and that measured chemically (PC) was somewhat biased by the presence of *G.echinulata* in the >12 μm size group (Figure 4). PC measurements obviously underestimated the biomass of this species. Estimated and measured carbon contents of the 2–12 μm size group, as well as those of the >12 μm group less *G.echinulata*, agreed fairly well. Measured values, however, always exceeded the estimated ones (Table I).

The carbon to chlorophyll ratio (C*/chl *a*) of the 3–12 μm fraction was unrealistically low (~20) in early May, and varied between 50 and 60 when *Rhodomonas* maintained a steady-state population at 90 μg C l^{-1} (Figures 3 and 5). The biomass of *Rhodomonas* might have been underestimated in May, therefore C* associated with this species was estimated in this time period as the chlorophyll *a* concentration in the 3–12 μm fraction, multiplied by 50. When the larger *Cryptomonas* became dominant, the C*/chl *a* ratios exceeded 100. After removing the effects of C*/chl *a* ratios and biomasses of *Rhodomonas* and *G.echinulata* from the ratio, a C*/chl *a* ratio of *Cryptomonas* could be estimated as 160–200 (Table I).

The C*/chl *a* ratios of the >12 μm group were calculated with *G.echinulata* excluded, for the reason that the relative pigment content of this species changed with limits of 30–300 μg C μg^{-1} chl *a* (Table I). C*/chl *a* ratios of the rest of the >12 μm size group were more variable than those of the smaller algae, and tended to decline during the summer (Figure 5).

The C*/chl *a* ratios showed an inverse relationship with the surface-to-volume ratios in both size groups, but were more pronounced in smaller algae. When their biomasses were the highest, the C*/chl *a* ratio of *A.formosa* could be estimated as 190, whereas that of *C.hirundinella* could be estimated as 300. C*/chl *a* ratios of five species could be calculated, and the relative chlorophyll contents decreased with the logarithm of the cell volumes ($r^2 = 0.80$; Table I).

Cell quotas and nutrient-related growth of the phytoplankton

P cell quotas (Q^*, μg P mg^{-1} C*) of the two size groups varied in a similar range, but showed different seasonal patterns (Figure 6). In early May, Q^*_{SP} of the 3–12 μm size group exceeded 10 μg P mg^{-1} C*. The high initial Q^*_{SP} quota decreased by 6.5% day^{-1} ($n = 8$, $r^2 = 0.97$) during the *Rhodomonas* dominance. In general, Q^*_{PP} followed a similar trend. Elevated P cell quotas were obtained during the *Cryptomononas* dominance. Variations of cell quotas, particularly those of Q^*_{SP} of the 3–12 μm algae, were largely independent of the epilimnetic SRP concentration.

In contrast to the small algae, variations of the P cell quotas in the >12 μm cells paralleled changes of the epilimnetic SRP concentration (cf. Figures 2 and 6), except that the cell quotas remained low during the early August SRP increase, when the lake mixed completely.

Growth rates (μ^*) varied between 0.03 and 0.82 day^{-1}, with essentially similar trends in both small and large organisms (Figure 6). Growth rates of the two algal size groups and those of the phytoplankton seemed to follow the Droop

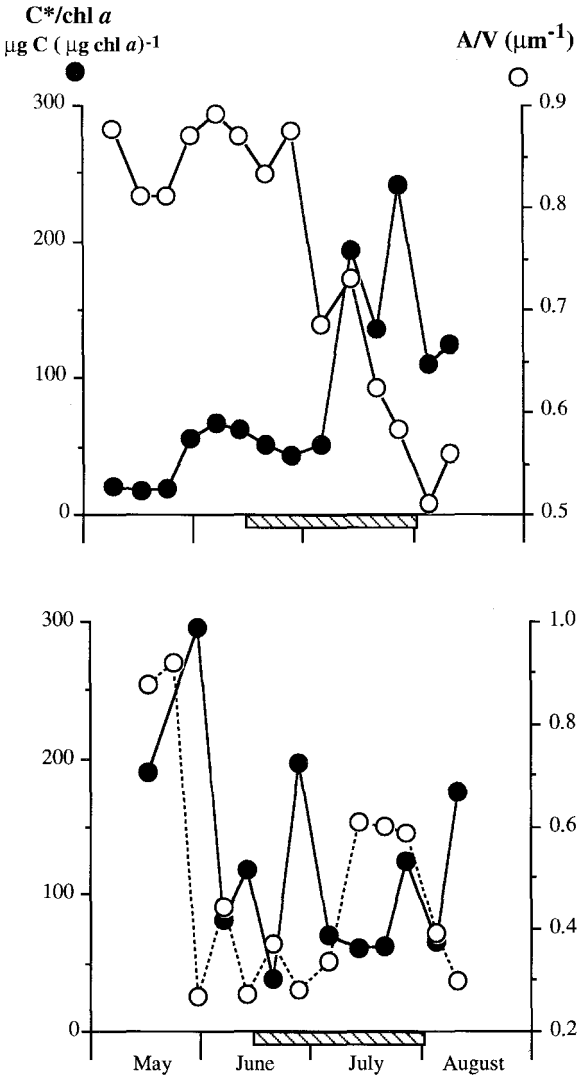

Fig. 5. Seasonal changes in the estimated carbon to chlorophyll *a* ratios and surface-to-volume (A/V) ratios. **Upper panel**: 3–12 µm algae; **lower panel**: >12 µm algae. (The period of permanent thermal stratification is shown on the horizontal axis.)

model when Q^*_{PP} cell quotas were used (Figure 7, Table III). The Q^*_{SP} quotas could be used for the community and for the >12 µm group, but not for the 3–12 µm algae. The Monod model was fitted to the estimated *in situ* phosphate concentrations (see below), but provided a less satisfactory description of the data, since growth seemed to cease at a threshold concentration of 0.4–0.5 µg P l^{-1} (Figure 7, Table III). The Monod model with SRP concentrations gave similar results.

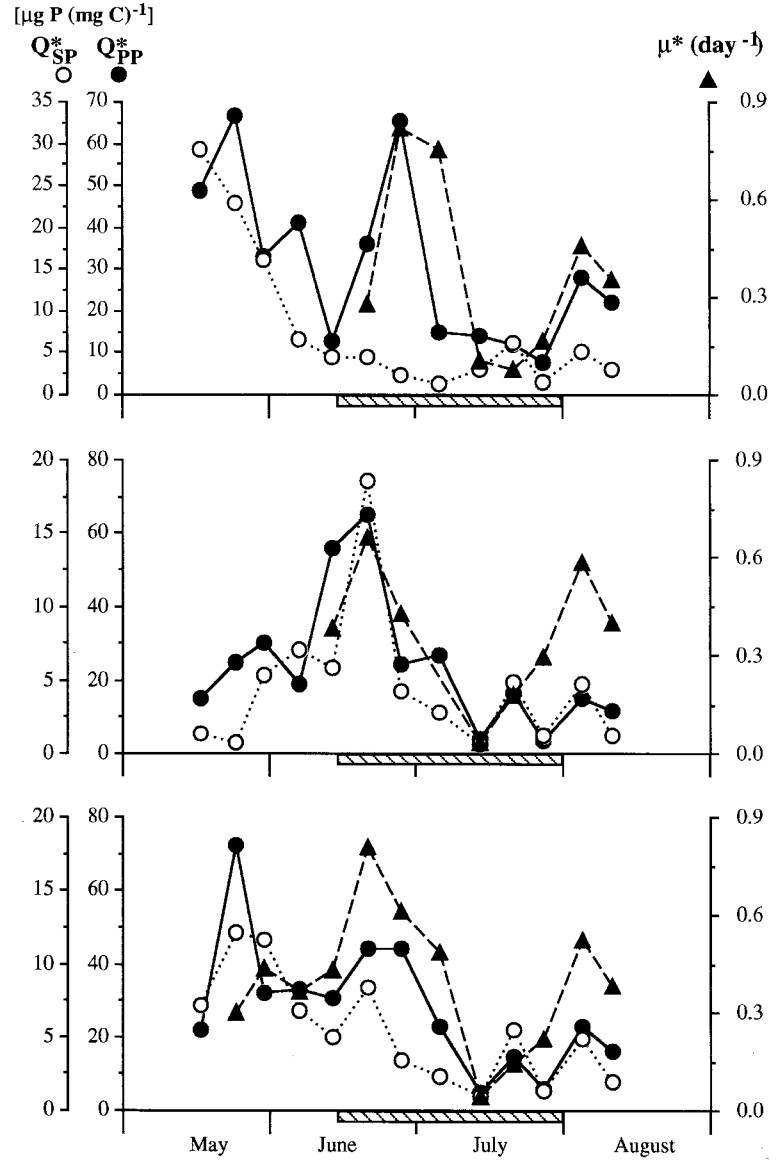

Fig. 6. Particulate (Q^*_{PP}) and surplus (Q^*_{SP}) P cell quotas, and growth rates (μ). **Upper panel**: 3–12 μm algae; **middle panel**: >12 μm algae; **lower panel**: community. (The period of permanent thermal stratification is shown on the horizontal axis.)

Larger algae had lower maximum specific growth rates ($\mu^*{}'_m$) and maintenance cell quotas ($Q^*_{PP,0}$) than smaller ones (Table II). $Q^*_{SP,0}$ made up 8% of $Q^*_{PP,0}$ in the >12 μm size group and 29% in the total phytoplankton (Table III).

Nitrogen cell quotas of the community were stable between 120 and 150 μg N

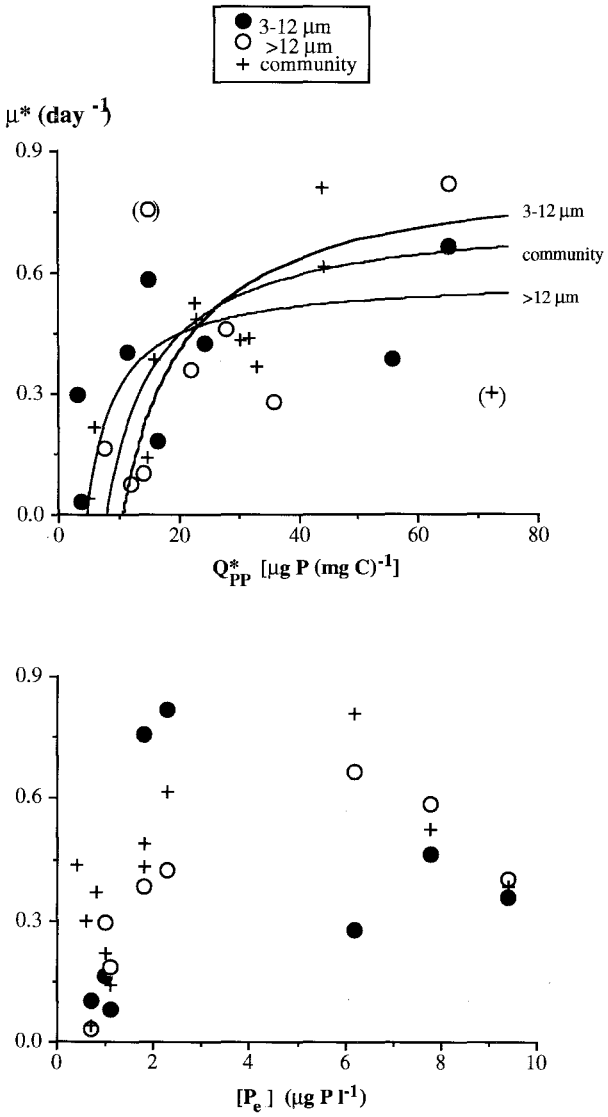

Fig. 7. Upper panel: Growth rate (µ) as a function of particulate P cell quota (Q^*_{PP}); Droop model. **Lower panel**: Growth rate as a function of estimated phosphate concentration ($[P_e]$); Monod model. (Points in parentheses were excluded from the regression.)

$mg^{-1}C$ before the bloom of the N_2-fixing cyanobacteria. Then the quotas increased to 170–180 µg N mg^{-1} C. Q_{PN} quotas of the two size groups were less stable and varied by a factor of about three. Although a limited number of data were available, the Droop model was also fitted with Q_{PN} quotas (Table III). Similar to P, smaller algae had higher $Q_{PN,0}$ values. The maintenance C:N:P ratio of the 3–12 µm size group was 93.7:8.6:1, whereas that of the >12 µm group was 215:12.5:1 by weight.

Table III. The constants of the Monod and Droop models

	3–12 μm	>12 μm	Community
Monod $[P_e]/\mu = K_s/\mu_m + [P_e]/\mu_m$			
μ_m (day^{-1})	0.399 ± 0.080	0.538 ± 0.104	0.503 ± 0.078
K_s (μg P l^{-1})	0.607 ± 1.195	0.827 ± 1.192	0.478 ± 0.743
r^2 [n]	0.831 [7]	0.842 [7]	0.821 [11]
Droop $\mu \times Q = \mu'_m \times Q - \mu'_m \times Q_0$			
μ'_m (day^{-1})	0.861 ± 0.133	0.583 ± 0.083	0.741 ± 0.101
$Q_{PP,0}$ (μg P mg^{-1} C)	10.67 ± 6.38	4.66 ± 5.35	8.09 ± 4.90
r^2 [n]	0.874 [8]	0.891 [8]	0.856 [11]
μ'_m (day^{-1})	–	0.685 ± 0.055	0.537 ± 0.111
$Q_{SP,0}$ (μg P mg^{-1} C)	–	1.36 ± 0.71	0.65 ± 1.31
r^2 [n]	–	0.963 [8]	0.721 [11]
μ'_m (day^{-1})	0.912 ± 0.251	0.452 ± 0.079	–
$Q_{PN,0}$ (μg N mg^{-1} C)	91.7 ± 85.5	58.1 ± 52.0	–
r^2 [n]	0.814 [5]	0.917 [5]	–

In principle, the intensity of nutrient limitation can be judged from the relative growth rates ($\mu^*/\mu^{*\prime}_m$). In June, prior to the onset of the thermal stratification, μ^* varied between 50 and 100% of $\mu^{*\prime}_m$ (Figure 8). Relative growth rates decreased to a minimum of 0.1 by mid-July, when *G.echinulata* dominated the plankton (cf. Figures 2 and 8). High relative rates were observed again at the end of the season.

Phosphate uptake by the phytoplankton

^{32}P uptake was relatively slow. Turnover times of orthophosphate in the water ranged between 1.3 and 3.0 h (mean 2.3 ± 0.6) during May and in late July, towards the end of the stratification period. In the rest of the season, much longer values were obtained (4.3–30.7 h, mean 18.6 ± 9.5). The pattern provided a good indicator of seasonal algal P deficiency (Figure 8).

The reciprocals of gross uptake rate constants increased with P additions (Woolf plot), but a negative departure was obvious at zero-added P, in harmony with the previous discussion (cf. Figures 1 and 9). The saturated P-uptake rate of the Michaelis–Menten model was estimated as the reciprocal of the linear regression line, with the systematically deviating value at zero-added P excluded.

Approximate gross P-uptake rates fitted reasonably to the Falkner model [equation (8), Figure 9, Thellier plot]. Kinetic parameters of gross and net P uptake were estimated according to equations (6)–(11) (Table IV).

On average, the initial phosphate concentration ($[P_e]_0$) exceeded the mean community threshold by a factor of 1.5 (Table IV). Seasonal averages of the threshold values were 0.47 ± 0.29 μg P l^{-1} in the 3–12 μm fraction and 0.75 ± 0.49 μg P l^{-1} in the >12 μm group, although occasionally higher values were estimated for smaller than for larger cells. $[P_e]_0$ obviously underestimated

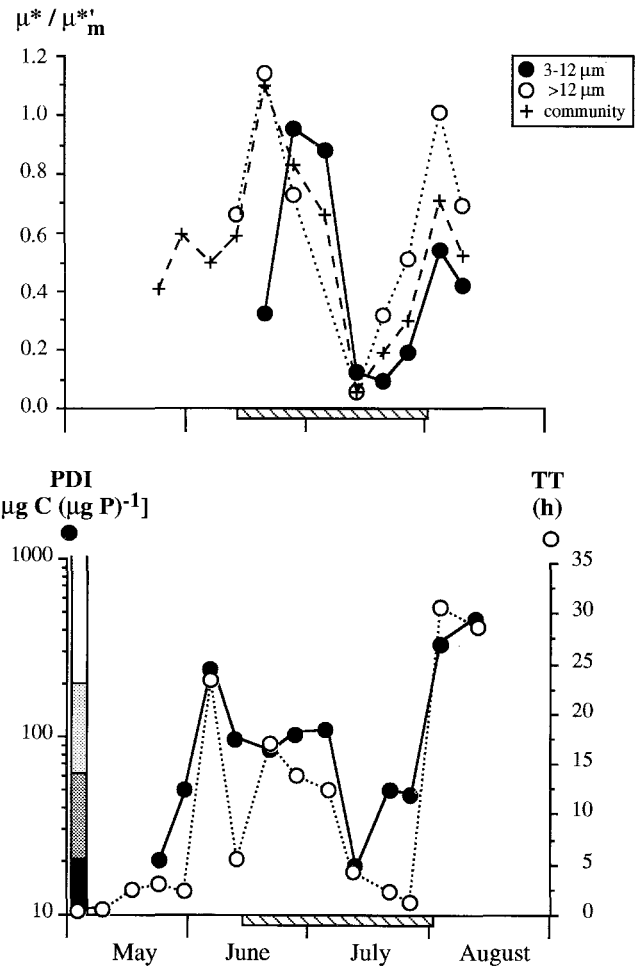

Fig. 8. Upper panel: Relative growth rates ($\mu^*/\mu^{*\prime}_m$) calculated from the Droop model. **Lower panel**: The Phosphorus Deficiency Indicator (PDI) and turnover time of orthophosphate in the water (TT). The left-hand scale indicates extreme (<20), moderate (20–60), low (60–200) and no (>200) P deficiency of algae based on PDI. (The period of permanent thermal stratification is shown on the horizontal axis.)

the peak SRP concentrations. In the rest of the season $[P_e]_0$ multiplied by 2.5 yielded values rather close to the measured SRP (Table IV, Figure 2). Chemical data were considered to approximate *in situ* P concentrations except in May, when even community average threshold concentrations exceeded the SRP values. At this time, the *in situ* P concentrations were estimated as $2.5 \times [P_e]_0$.

Conductivity coefficients were normalized to estimated cell carbon with *G.echinulata* excluded. The specific conductivity coefficient decreased with the improving P status of the algae, and with the decreasing surface-to-volume ratios. Larger cells had a 1.5–44 times higher carbon-specific conductivity coefficient than smaller ones (Table IV). A similar difference could be seen in

Table IV. Kinetic constants of the linear force–flow model of Falkner *et al.* (1989)

Date	3–12 μm			>12 μm			Community			$[P_e]_0$	*In situ* $[P_e]$
	L_P	$[P_e]_T$	$[P'_e]_T$	L_P	$[P_e]_T$	$[P'_e]_T$	L_P	$[P_e]_T$	$[P'_e]_T$		
8 May	–	–	–	–	–	–	0.987	0.490	0.177	0.490	1.2
16 May	–	–	–	1.239	0.486	0.375	0.986	0.593	0.126	0.347	0.9
23 May	0.711	0.243	0.007	2.040	0.354	0.248	1.610	0.357	0.096	0.226	0.6
29 May	0.665	0.381	0.076	1.008	0.304	0.087	0.954	0.299	0.065	0.175	0.4
5 June	0.063	0.474	0.021	0.280	0.717	0.495	0.153	0.538	0.120	0.332	0.8
12 June	0.265	0.097	0.028	0.631	0.347	0.244	0.380	0.108	0.037	0.107	1.8
19 June	0.201	0.911	0.053	3.870	0.983	0.560	0.984	0.995	0.359	0.718	6.2
26 June	–	–	–	0.776	1.242	0.260	0.491	1.144	0.253	0.689	2.3
7 July	–	–	–	–	–	–	0.491	1.280	0.266	0.704	1.8
11 July	–	–	–	–	–	–	0.618	0.501	0.174	0.514	0.7
19 July	0.040	0.714	0.0004	1.779	0.681	0.387	0.663	0.727	0.185	0.503	1.1
25 July	0.259	0.174	0.029	0.710	0.704	0.497	0.332	0.268	0.074	0.198	1.0
2 August	0.154	0.727	0.291	0.430	1.957	0.899	0.163	1.097	0.260	0.699	7.8
8 August	–	–	–	–	–	–	0.076	1.018	0.255	0.704	9.4

L_P = specific conductivity coefficient (μg P mg^{-1} C h^{-1}); $[P_e]_T$, $[P'_e]_T$, $[P_e]_0$ and *in situ* $[P_e]$ are the threshold, apparent threshold, initial and *in situ* phosphate concentrations (μg P l^{-1}), respectively.

conductivity coefficients normalized to unit cell surface (Table I). The seasonal averages were 1.28 ± 1.07 μg P mg^{-1} C h^{-1} or 0.41 ± 0.40 × 10^{-9} μg P μm^{-1} h^{-1} in the >12 μm size group, and 0.29 ± 0.26 μg P mg^{-1} C h^{-1} or 0.09 ± 0.07 × 10^{-9} μg P μm^{-1} h^{-1} in the 3–12 μm group. In spite of the higher P-uptake activity of the larger cells, larger algae never incorporated >50% of ^{32}P at zero-added P (Figure 9), and their contribution to the ^{32}P incorporation was disproportionately low in comparison to their biomass.

The conductivity coefficient was highly correlated with the saturated rate of P uptake ($n = 13$, $r^2 = 0.99$), and its numeric value was one half of the latter. This close agreement allowed the Phosphorus Deficiency Indicators (PDI) to be calculated as the maximum rate of photosynthesis divided by the conductivity coefficient of P uptake, although PDI has originally been derived from the substrate-saturated rate of P uptake (Lean and Pick, 1981). PDI ranged between 20 and 500, and was indicative of moderate to low P deficiency (Figure 8). PDI, turnover times and $\mu^*/\mu^{*\prime}_m$ ratios showed similar temporal patterns. PDI was correlated with the exstimated *in situ* P concentration ($n = 10$, $r^2 = 0.99$).

Instantaneous specific net P-uptake rates (v^*_{net}, μg P mg^{-1} C day^{-1}) were calculated from the kinetic constants of the Falkner model [equation (4)] with the estimated *in situ* P concentrations and with the assumption that P uptake went on during the whole day. These data were compared with steady-state specific P uptake rates [u^*_P, μg P mg^{-1} C day^{-1}; equation (3)]. Instantaneous rates were normalized to cell carbon minus carbon associated with *G.echinulata*. Since neither P quotas nor carbon-fixation data were available for *G.echinulata* alone, steady-state rates had to be normalized to total estimated carbon. When size-fractionated production data were not available, growth rates of the two algal groups were estimated from the constants of the Droop model by using the size-fractionated Q_{PP} values (Figure 10). The two data sets showed very similar seasonal patterns in both the community and the >12 μm algae.

Discussion

Species composition and growth

In Lake Erken, the thermal stratification developed late, and it was short-lasting and unstable during the summer of 1989 (Figure 2; Pierson *et al.*, 1992). Compared to summers with more stable thermal structures, relatively more of the internal P loading (~3 mg P m^{-2} day^{-1}) was associated with epilimnetic SRP inputs than with upward migration of P-rich *G.echinulata* colonies from the sediments to the epilimnion (Pettersson *et al.*, 1990, 1993; Pierson *et al.*, 1992; Istvánovics *et al.*, 1993). As a consequence of the sufficient P supply, algal P deficiency was moderate to low (Figure 8; Istvánovics *et al.*, 1992).

Although the resource competition was not sharp, the species composition of phytoplankton followed the general summer successional patterns (Reynolds, 1989; Sommer, 1989a). Fast-growing, r-selected species (primarily *R.minuta*) dominated early in the season (Figure 3). Larger, K-selected species (e.g. *C.hirundinella*) were favored by more stable physical conditions. A bloom of N_2-fixing cyanobacteria (*G.echinulata* and *A.circinalis*) coincided with minimum

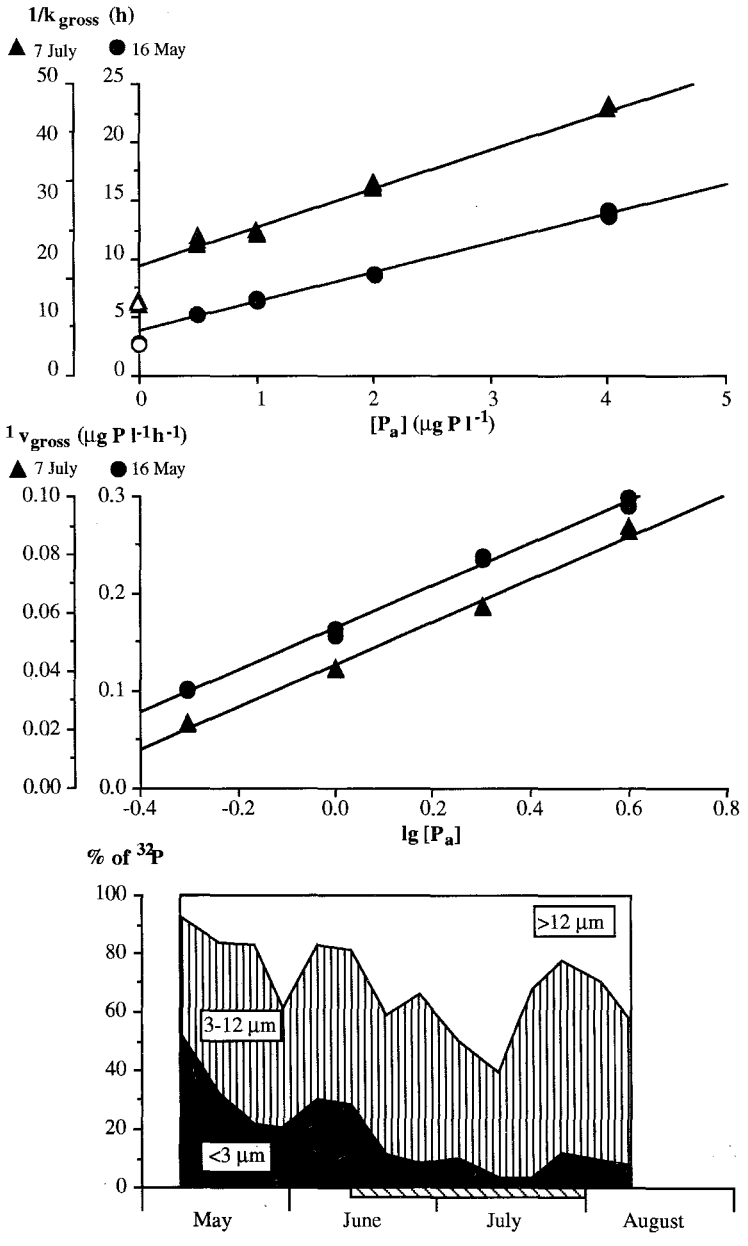

Fig. 9. Upper panel: Reciprocals of gross P-uptake rate constants (k_{gross}) plotted against the orthophosphate addition, [P_a] (Woolf plot, Michaelis–Menten model). Open symbols were excluded from the regression. (16 May: $1/k_{gross} = 3.67 + 2.48\ [P_a]$, $n = 8$, $r^2 = 1.00$; 7 July: $1/k_{gross} = 18.67 + 6.63\ [P_a]$, $n = 8$, $r^2 = 1.00$.) **Middle panel**: Approximate gross P-uptake rates ($^1v_{tross}$) plotted against log[P_a] (Thellier plot, Falkner model). (16 May: $^1v_{gross} = 0.165 + 0.217 \log[P_a]$, $n = 8$, $r^2 = 1.00$; 7 July: $^1v_{gross} = 0.042 + 0.073 \log[P_a]$, $n = 8$, $r^2 = 0.99$.) **Lower panel**: Size distribution of ^{32}P uptake at [P_a] = 0. (The period of permanent thermal stratification is shown on the horizontal axis.)

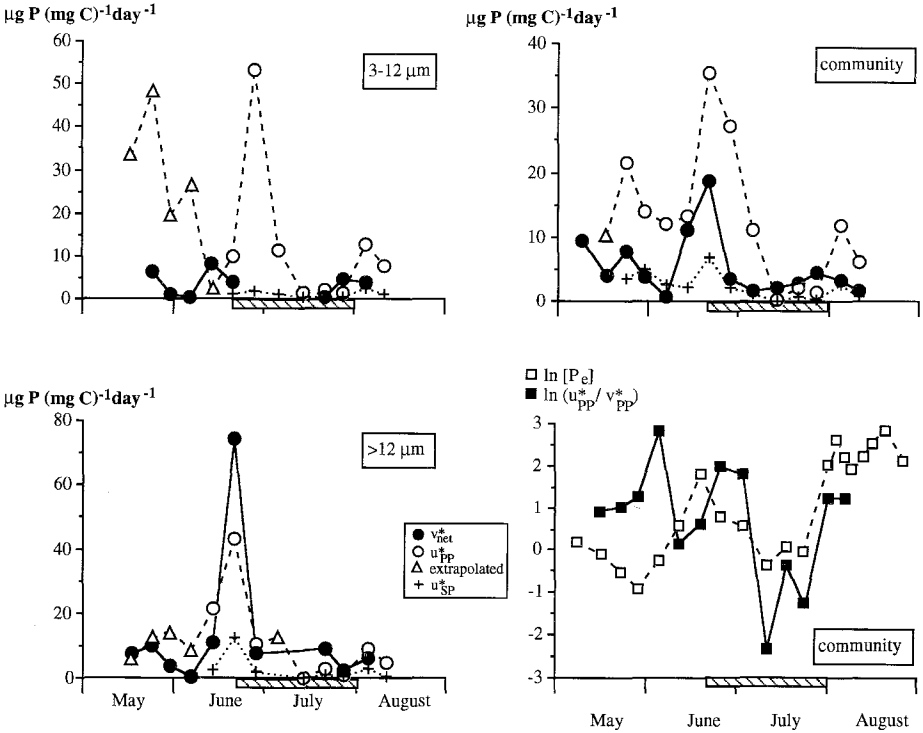

Fig. 10. Specific instantaneous (v^*_{net}) and steady-state (u^*_{PP}, u^*_{SP}) net P-uptake rates of the two algal size groups and those of the community. When photosynthetic rates were not measured, u^*_{PP} values were extrapolated from Q^*_{PP} data using the constants of the Droop model (Table III). The right-hand lower graph indicates the *in situ* phosphate concentration ($[P_c]_0$) and the ratio of u^*_{PP}/v^*_{net}. (The period of permanent thermal stratification is shown on the horizontal axis.)

DIN/SRP ratios. Relatively high abundance of summer diatoms (*A.formosa*, *Stephanodiscus* spp. and small Centrales) was indicative of the unstable physical conditions.

In general, net rates of biomass changes of the dominant species were similar to the corresponding values from Lake Constance (Sommer, 1981; Table II). Net growth rates of cryptophytes were comparatively low. *Rhodomonas* is highly susceptible to zooplankton grazing (Nauwerck, 1963; Reynolds *et al.*, 1984; Braunwarth and Sommer, 1985), and its population might have been controlled by grazing during this study, too.

In 1989, just as in recent summer studies in Lake Erken (Istvánovics *et al.*, 1990; Pettersson *et al.*, 1993; Bell *et al.*, 1994), partitioning of chlorophyll *a*, algal ^{14}C uptake and bacterial [^{3}H]thymidine incorporation showed that bacteria and phytoplankton were fairly well, but not completely, separated by 3 µm membrane filters. Microscopic enumeration of phytoplankton revealed that 12 µm membrane filters separated sufficiently the dominant r- and K-selected algal species.

Carbon estimated from cell counts (C*) paralleled PC values measured chemically (Figure 4). The former data were considered to be more reliable for

two reasons. First, carbon associated with >200 μm *G.echinulata* colonies was obviously underestimated by chemical measurements (Figure 4). The reason is that the number of colonies is low even during a heavy bloom (<200 l^{-1}), and a representative sampling is not possible unless colonies are concentrated from a large volume of water. Second, detrital carbon is ~100 μg l^{-1} in the epilimnion of Lake Erken (Pettersson, 1980), with the largest interference in the >12 μm fraction (Figure 4; Pettersson *et al.*, 1993).

The ratio of C* to chlorophyll *a* was a further indication that our C* values were acceptable estimates (Figure 5; cf. Harris, 1986). The inverse relationship between relative chlorophyll contents and cell volumes of the dominant species (Table I) was in harmony with the observation that smaller species are richer in chlorophyll than larger ones (Vörös and Padisák, 1991).

P cell quotas and growth rates showed similar seasonal patterns, minima being observed during the *G.echinulata* bloom (Figure 6). An intense study in 1991 revealed that both cell quotas and maximum growth rates of the epilimnetic colonies of this species were low (Q_{PP} = 5–10; Q_{SP} = 1.4 μg P mg^{-1} C; μ'_m = 0.37 ± 0.04 day^{-1}; Istvánovics *et al.*, 1993). Pierson *et al.* (1992) observed that chlorophyll-specific rates of photosynthesis invariably fell to a minimum in different years during the *G.echinulata* bloom. Given the obvious species-specific dependence of both P cell quotas and growth rates, the Droop model described algal growth surprisingly well (Figures 6 and 7, Table III). The Droop model failed only with the Q^*_{SP} cell quotas of the 3–12 μm algae, as it did in a cryptophyte-dominated Norwegian lake (Vadstein *et al.*, 1988).

Sommer (1989b) concluded that the *in situ* $Q_{PP,0}$ quotas of various co-existing species were similar and ~3 μg P mg^{-1} C. In contrast to this, other field studies revealed distinct interspecific differences in the maintenance cell quotas (Sakshaug *et al.*, 1983; Harris, 1986). In Lake Erken, $Q^*_{PP,0}$ of the 3–12 μm size fraction was significantly higher than that of the >12 μm group (Table III, Figure 6).

The estimated $Q^*_{SP,0}$ was 1.4 μg P mg^{-1} C in the >12 μm algae and 0.62 μg P mg^{-1} C in the community. These values were lower than that which Fitzgerald and Nelson (1966) suggested to be indicative of P deficiency (1.6 μg P mg^{-1} C], and which Pettersson (1980) found to be actually indicative of such conditions in Lake Erken during the spring (2 μg P mg^{-1} C). Minimum measured Q^*_{PP} and Q^*_{SP} cell quotas near the estimated maintenance values, minimum growth rates and, consequently, minimum relative growth rates ($\mu^*/\mu^{*\prime}_m$ = 0.1!, Figure 8) all coincided with the *G.echinulata* bloom when, however, PDI, a superior indicator of algal P status (Istvánovics *et al.*, 1992), showed not more than moderate P deficiency at this time (Figure 8). This discrepancy reflects the influence of the shift in the species composition discussed above, and clearly illustrates that even though the Droop model can be used to describe phytoplankton growth with some degree of success, interpretation of the results is not always straightforward.

In 1989, photosynthesis by *G.echinulata* was not measured. During its 1991 bloom, chlorophyll-specific rates of light-saturated photosynthesis increased gradually from ~2 μg C μg^{-1} chl *a* h^{-1} to ~6 μg C μg^{-1} chl *a* h^{-1} in the rest of

the phytoplankton (D.C.Pierson, unpublished). This supports the conclusion that very low relative community growth rates in the second half of July 1989 reflected the dominance of a slow-growing species, rather than low relative growth rates of other co-existing species. Some decrease in the relative growth rates of other species might have occurred though, since the cyanobacterial bloom decreased the depth of the euphotic zone below the mixing depth (Figure 2).

Minimum nitrogen cell quotas were also estimated for the two size groups by the Droop model. Smaller algae required not only more P, but also more N for their growth. The minimum C:N:P weight ratios were close to the 'depletion line' in a C:P and N:P space (Harris, 1986). This, together with the DIN/SRP ratios (Figure 2), suggests that neither could N availability seriously limit growth of the phytoplankton in Lake Erken.

In Lake Erken, the relationship between the external P concentrations and growth rates seemed to be more complicated than predicted by the simple Monod model (Figure 7, Table III). Relatively low growth rates at high P concentrations were probably associated with changes in the species composition. Besides, growth seemed to cease at a threshold concentration (Figure 7). Auer *et al.* (1986) obtained better fits to the Monod model modified for a substrate threshold than to the original model in Green Bay, Lake Michigan. The SRP threshold was 0.5 ± 0.4 μg P l^{-1} in that study. Our data set was too small to fit the modified model, but a qualitatively similar threshold could be estimated.

The original Monod model may apply under a restricted set of growth conditions. Chemostat experiments showed that growth ceased at a species-specific substrate threshold (Button, 1985). Unlike the Monod model, the Droop model is in harmony with the threshold behavior of both growth and P uptake (Button, 1985; Falkner *et al.*, 1989), and implies the possible time lag between the two processes.

Phosphate uptake

^{32}P uptake kinetics followed the linear force–flow model of Falkner *et al.* (1989) (Figure 9), similar to other lakes (Falkner and Falkner, 1989; Istvánovics and Herodek, 1995), and to the P uptake by *G.echinulata* (Istvánovics *et al.*, 1993). Since the threshold of *G.echinulata* was permanently >10 μg P l^{-1}, and the large colonies accumulated negligible ^{32}P below an external P concentration of 5 μg P l^{-1} (Istvánovics *et al.*, 1990), we assumed that this species did not contribute to the isotope incorporation under the conditions of the present study.

Net P-uptake rates were estimated according to Istvánovics and Herodek (1995). This approach has been developed for extremely P-deficient planktonic microorganisms of Lake Balaton, where it could justifiably be assumed that no net P uptake occurred at zero-added P. Phytoplankton in Lake Erken, however, were less P deficient. Net uptake certainly took place in unenriched samples, at least at peak SRP concentrations. When $v_{net} > 0$ at $[P_a] = 0$, the above approach may still be used. However, a significant difference is that the $\log[P_c]$

axis is shifted upwards in Figure 1, so that the intercept of the community average uptake curve on the abscissa remains at $[P_e]_0$. This transformation shifts both the thresholds and apparent thresholds to larger values, but leaves the conductivity coefficient unchanged. Leakage rates will be overestimated with a corresponding underestimation of the net uptake rates. If $[P_e]_0$ exceeded thresholds of each species, no deviation could be observed at $[P_a] = 0$ on a Woolf plot, and the estimated $[P_e]_0$ and community $[P_e]_T$ values were equal. This occurred in Lake Erken on 12 June and 11 July (Table IV).

The discrepancy between kinetic and chemical data at the SRP peaks remains unresolved. On the one hand, in these periods SRP exceeded $[P_e]_0$ by a factor of 15–20 (Table IV). The traditional bioassay of Rigler (1966) revealed that chemical data were much too high, whereas $[P_e]_0$ would be an acceptable estimate of the orthophosphate concentration (Figure 11). ^{32}P-uptake kinetics could be recalculated from the kinetic constants of the Falkner model (Figure 11). ^{32}P uptake was so slow that even if the isotope incorporation were only due to net uptake (leakage were zero), the original SRP concentration of 6.2 μg P l^{-1} on 19 June could not be decreased below 1.6 μg P l^{-1} in 24 h. On the other hand, there is no reason to believe that chemical overestimation of the real orthophosphate concentration was more serious during the SRP peaks than at low SRP concentrations. Continuously registered physical conditions, high hypolimnetic SRP concentrations and low algal P deficiency all support the contention that significant phosphate inputs occurred to the epilimnion when peak SRP values were observed (Istvánovics *et al.*, 1992; Pierson *et al.*, 1992; Pettersson *et al.*, 1993).

Community average thresholds in Lake Erken (Table IV) exceeded by an order of magnitude the thresholds of P-depleted chemostat cultures (Falkner *et al.*, 1989), and the community thresholds of extremely P-deficient spring plankton in Lake Balaton (Istvánovics and Herodek, 1995). In spite of the similar chlorophyll concentrations, the conductivity coefficients in μg P l^{-1} h^{-1} units were lower in Lake Erken than in the latter lake by a factor of 10–100. The high thresholds and low conductivity coefficients reflected relatively good P supply of the phytoplankton in Lake Erken. The large difference between the two lakes clearly supports the theory of Falkner *et al.* (1989), that micro-organisms adjust their uptake characteristics to the external P concentration, so that assimilation will always proceed with optimum efficiency. Increased P concentration leads to decreased transport activity which, in turn, results in an elevated threshold value.

In general, smaller algae had only slightly lower thresholds than larger ones (Tables I and IV). The 3–12 μm fraction was dominated by cryptophytes, which grow preferentially in nutrient-rich environments (Reynolds *et al.*, 1984; Sommer, 1986; Reynolds, 1988). Their half-saturation constants of P uptake are relatively high: that of *Cryptomonas erosa* was 4 μg P l^{-1} (Smith and Kalff, 1983), whereas that of *Rhodomonas lacustris* reached 12 μg P l^{-1} (Brekke, 1987). Therefore, the similar range of thresholds of the two algal groups in Lake Erken seemed to be realistic.

As expected (Reynolds, 1989), carbon-specific conductivity coefficients of the

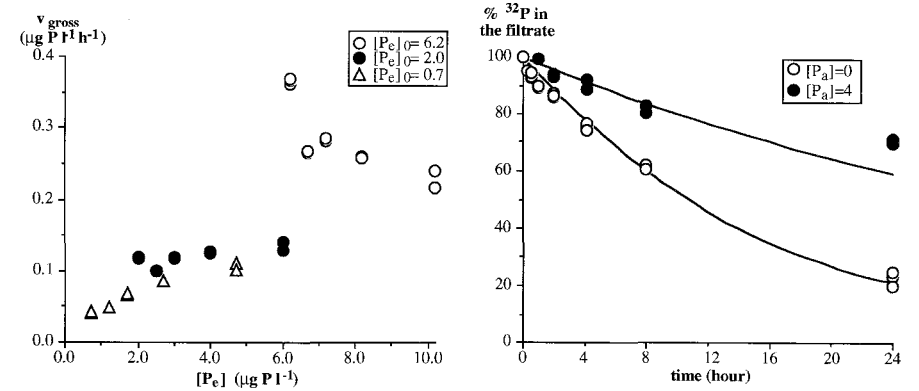

Fig. 11. Left panel: Gross P-uptake rates (v_{gross}) estimated with different initial phosphate concentrations ($[P_e]_0$) on 19 June. $[P_a]$ = phosphate addition. $[P_e]_0$ = 0.7 µg P l^{-1} estimated from the Falkner model is acceptable, the measured SRP concentration (6.2 µg P l^{-1}) is too high. **Right panel**: The decrease in ^{32}P radioactivity in the filtrate of 0.2 µm membrane filters on 19 June. Symbols represent measured data, lines were recalculated from the constants of the Falkner model (Table IV).

community and those of the two size fractions were inversely related to the respective surface-to-volume ratios (cf. Figure 5 and Table IV). However, larger algae had, on an average, four times higher conductivity coefficients both per unit cell carbon and per unit cell surface. The explanation provided by Falkner's model is that the maintenance of similar thresholds was more expensive in energetic terms for larger than for smaller algae.

If the thresholds of the two groups were identical, higher P-uptake activities of larger cells would result in higher net P uptake rates relative to smaller cells [equation (4)]. The difference in the fractional thresholds was not sufficiently large to alter this picture significantly and, consequently, to account for a disproportionately low contribution of large algae to ^{32}P incorporation at $[P_a] = 0$ (Figure 9). It is a higher leakage from smaller cells relative to larger ones that may account for this partitioning pattern. Indeed, seasonal averages of carbon-specific leakage rates were 0.19 ± 0.18 µg P mg^{-1} C h^{-1} in the >12 µm group and 0.40 ± 0.46 µg P mg^{-1} C h^{-1} in the 3–12 µm group. Since net uptake might occur at zero added P, the absolute values are not decisive, but the ratio may be realistic. Other investigators also concluded that larger and/or more 'complex' organisms reduced their leakage rates more efficiently than smaller ones (Lean and Nalewajko, 1976; Lehman and Sandgren, 1982; Lean and White, 1983; Istvánovics and Herodek, 1995). A reduced leakage increases the growth efficiency and simultaneously results in a decreased P-uptake threshold (Falkner *et al.*, 1989).

The typical ^{32}P incorporation patterns by other, more P-deficient communities are much more pronounced in favor of bacterial sized cells than they were in the present study (Lean and White, 1983; Currie and Kalff, 1984). Noticeably, the share of the smallest microorganisms (<3 µm) was higher (40–75%) during August 1988 in Lake Erken (Istvánovics *et al.*, 1990), when exceptionally stable

thermal stratification resulted in larger P deficiency of the plankton as compared to 1989 (Istvánovics *et al.*, 1992; Pierson *et al.*, 1992).

Instantaneous and steady-state net P-uptake rates

The assumptions behind estimating net P-uptake rates from ^{32}P uptake data result in community threshold values that are higher than, or equal to $[P_e]_0$ (Figure 1). The Falkner model [equation (4)] will then predict net P release from the cells. This is obviously not the *in situ* situation with species in their growth phases. Further assumptions are necessary to interpret laboratory data under field conditions.

We illustrate the problem on the example of large (600 km^2) shallow (Z_{mean} = 3.1 m) Lake Balaton with its extremely P-deficient planktonic microorganisms (Istvánovics and Herodek, 1995). Let the *in situ* P concentration be low, but higher than the $[P_e]_0$, at which net uptake of each species ceases (Figure 1). Wind-induced sediment resuspension, followed by P desorption, is a principal P supply in such large and shallow lakes. This supply, however, is inevitably cut off by the containment of a water sample. Depending on the transport activity, the P concentration in the sample may rapidly be depleted to $[P_e]_0$. With the assumption that the *in situ* P concentration exceeded $[P_e]_0$ by a factor of four, 30–120 min were enough to exhaust the available P pool in an enclosed water sample from Lake Balaton.

The situation was dramatically different in Lake Erken. Leakage rates were most probably overestimated at $[P_a] = 0$, since net P uptake might occur even in unenriched samples. If it were so, $[P_e]_0$ might be a better measure of the *in situ* phosphate concentrations in Lake Erken than in Lake Balaton. One should assess, then, how much the real threshold values were overestimated. Since the net uptake rate is proportional to the $[P_e]/[P_e]_T$ ratio [equation (4)], a lower $[P_e]_T$ or a higher $[P_e]_0$ causes equivalent transformations to v_{net}. A value of 2.5 $\times$ $[P_e]_0$ was most often fairly close to the measured SRP concentrations (Table IV). Therefore, chemical data were used to estimate '*in situ*' instantaneous net uptake rates. However, it must be emphasized that in Lake Erken the $[P_e]_0$ rather than chemical data might estimate the *in situ* orthophosphate concentrations, and most probably the thresholds were lower.

Given all the uncertainties and oversimplifications which both our u^*_P and v^*_{net} estimates include, the similarity of their seasonal trends is really surprising (Figure 10). Noticeably, the two rate estimates were truly independent and shared only a single common variable; both of them were normalized to cell carbon. This suggests that our approach of estimating net P uptake rates from ^{32}P-uptake kinetics is not meaningless.

Higher instantaneous than steady-state uptake rates would indicate that organisms consume nutrients in excess of their immediate growth requirements and, vice versa, steady-state rates would exceed instantaneous rates when algae grow at the expense of their accumulated nutrient reserves. In this study, the steady-state rates might be too high since they were calculated from light-saturated gross photosynthesis rates. On the contrary, instantaneous rates might

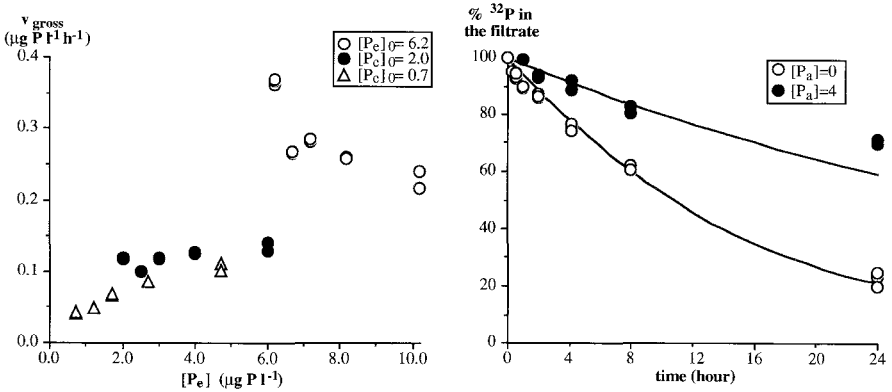

Fig. 11. Left panel: Gross P-uptake rates (v_{gross}) estimated with different initial phosphate concentrations ($[P_c]_0$) on 19 June. $[P_a]$ = phosphate addition. $[P_c]_0$ = 0.7 µg P l^{-1} estimated from the Falkner model is acceptable, the measured SRP concentration (6.2 µg P l^{-1}) is too high. **Right panel**: The decrease in ^{32}P radioactivity in the filtrate of 0.2 µm membrane filters on 19 June. Symbols represent measured data, lines were recalculated from the constants of the Falkner model (Table IV).

community and those of the two size fractions were inversely related to the respective surface-to-volume ratios (cf. Figure 5 and Table IV). However, larger algae had, on an average, four times higher conductivity coefficients both per unit cell carbon and per unit cell surface. The explanation provided by Falkner's model is that the maintenance of similar thresholds was more expensive in energetic terms for larger than for smaller algae.

If the thresholds of the two groups were identical, higher P-uptake activities of larger cells would result in higher net P uptake rates relative to smaller cells [equation (4)]. The difference in the fractional thresholds was not sufficiently large to alter this picture significantly and, consequently, to account for a disproportionately low contribution of large algae to ^{32}P incorporation at $[P_a] = 0$ (Figure 9). It is a higher leakage from smaller cells relative to larger ones that may account for this partitioning pattern. Indeed, seasonal averages of carbon-specific leakage rates were 0.19 ± 0.18 µg P mg^{-1} C h^{-1} in the >12 µm group and 0.40 ± 0.46 µg P mg^{-1} C h^{-1} in the 3–12 µm group. Since net uptake might occur at zero added P, the absolute values are not decisive, but the ratio may be realistic. Other investigators also concluded that larger and/or more 'complex' organisms reduced their leakage rates more efficiently than smaller ones (Lean and Nalewajko, 1976; Lehman and Sandgren, 1982; Lean and White, 1983; Istvánovics and Herodek, 1995). A reduced leakage increases the growth efficiency and simultaneously results in a decreased P-uptake threshold (Falkner *et al.*, 1989).

The typical ^{32}P incorporation patterns by other, more P-deficient communities are much more pronounced in favor of bacterial sized cells than they were in the present study (Lean and White, 1983; Currie and Kalff, 1984). Noticeably, the share of the smallest microorganisms (<3 µm) was higher (40–75%) during August 1988 in Lake Erken (Istvánovics *et al.*, 1990), when exceptionally stable

thermal stratification resulted in larger P deficiency of the plankton as compared to 1989 (Istvánovics *et al.*, 1992; Pierson *et al.*, 1992).

Instantaneous and steady-state net P-uptake rates

The assumptions behind estimating net P-uptake rates from ^{32}P uptake data result in community threshold values that are higher than, or equal to $[P_e]_0$ (Figure 1). The Falkner model [equation (4)] will then predict net P release from the cells. This is obviously not the *in situ* situation with species in their growth phases. Further assumptions are necessary to interpret laboratory data under field conditions.

We illustrate the problem on the example of large (600 km^2) shallow (Z_{mean} = 3.1 m) Lake Balaton with its extremely P-deficient planktonic microorganisms (Istvánovics and Herodek, 1995). Let the *in situ* P concentration be low, but higher than the $[P_e]_0$, at which net uptake of each species ceases (Figure 1). Wind-induced sediment resuspension, followed by P desorption, is a principal P supply in such large and shallow lakes. This supply, however, is inevitably cut off by the containment of a water sample. Depending on the transport activity, the P concentration in the sample may rapidly be depleted to $[P_e]_0$. With the assumption that the *in situ* P concentration exceeded $[P_e]_0$ by a factor of four, 30–120 min were enough to exhaust the available P pool in an enclosed water sample from Lake Balaton.

The situation was dramatically different in Lake Erken. Leakage rates were most probably overestimated at $[P_a] = 0$, since net P uptake might occur even in unenriched samples. If it were so, $[P_e]_0$ might be a better measure of the *in situ* phosphate concentrations in Lake Erken than in Lake Balaton. One should assess, then, how much the real threshold values were overestimated. Since the net uptake rate is proportional to the $[P_e]/[P_e]_T$ ratio [equation (4)], a lower $[P_e]_T$ or a higher $[P_e]_0$ causes equivalent transformations to v_{net}. A value of 2.5 $\times$ $[P_e]_0$ was most often fairly close to the measured SRP concentrations (Table IV). Therefore, chemical data were used to estimate '*in situ*' instantaneous net uptake rates. However, it must be emphasized that in Lake Erken the $[P_e]_0$ rather than chemical data might estimate the *in situ* orthophosphate concentrations, and most probably the thresholds were lower.

Given all the uncertainties and oversimplifications which both our u^*_P and v^*_{net} estimates include, the similarity of their seasonal trends is really surprising (Figure 10). Noticeably, the two rate estimates were truly independent and shared only a single common variable; both of them were normalized to cell carbon. This suggests that our approach of estimating net P uptake rates from ^{32}P-uptake kinetics is not meaningless.

Higher instantaneous than steady-state uptake rates would indicate that organisms consume nutrients in excess of their immediate growth requirements and, vice versa, steady-state rates would exceed instantaneous rates when algae grow at the expense of their accumulated nutrient reserves. In this study, the steady-state rates might be too high since they were calculated from light-saturated gross photosynthesis rates. On the contrary, instantaneous rates might

be too low and, anyway, their numeric value depends on the choice of the *in situ* P concentration. As a consequence, the two estimates are not comparable in absolute terms; the seasonal trend of their ratio is more instructive (Figure 10).

During the developing thermal stratification in May (Figure 2), the epilimnetic SRP pool has been depleted and algae were moderately P deficient (Figure 8). High u^*_P/v^*_{net} ratios indicated that utilization of stored P might be necessary to maintain algal growth.

High turbulence in June, prior to the onset of the permanent thermal stratification, resulted in a gradual SRP increase in the euphotic zone. The inputs were sufficiently large to ease algal P deficiency (Figure 8), as well as to replenish the intracellular P reserves. Cell quotas increased (Figure 6), u^*_P/v^*_{net} ratios were low (Figure 10).

After the onset of the permanent thermal stratification, epilimnetic SRP was depleted again. Diminishing P cell quotas (Figure 6) and increasing u^*_P/v^*_{net} ratios (Figure 10) showed that stored P had to be converted to new biomass. By mid-July, phytoplankton became moderately P deficient (Figure 8). *Gloeotrichia echinulata*, this slow-growing cyanobacterium, gradually took over the dominance (Figure 3). Epilimnetic growth of this species is based solely on stored P (Istvánovics *et al.*, 1993). This shift in the species composition was more likely driven by physical conditions than by other factors, including nutrients (cf. Pierson *et al.*, 1992; Istvánovics *et al.*, 1993).

Gradual erosion of the epilimnion after mid-July resulted in enhanced P supply rates to the epilimnion. Epilimnetic SRP increased, low u^*_P/v^*_{net} ratios indicated replenishment of the P reserves (Figure 10) and algae recovered from their slight P deficiency (Figure 8).

Acknowledgements

V.Istvánovics was supported as guest researcher by the Erken Laboratory. Her work was partly financed by grant no. 1884 of the Hungarian National Research Foundation (OTKA). We thank E.Szász, U.Lindquist and T.Waara for technical assistance.

List of symbols

Chemical parameters

SRP, SP, PP, TP—soluble reactive, surplus, particulate and total phosphorus ($\mu g\ P\ l^{-1}$)
DIN—dissolved inorganic nitrogen ($\mu g\ N\ l^{-1}$)
PC—measured particulate carbon ($\mu g\ C\ l^{-1}$)
C*—carbon estimated from algal cell counts ($\mu g\ C\ l^{-1}$)

Growth

P_m—light-saturated rate of photosynthesis ($\mu g\ C\ l^{-1}\ h^{-1}$)
μ—specific growth rate (day^{-1})

μ_m, μ'_m—maximum specific growth rate at infinite external and internal substrate concentrations, respectively (day^{-1})
K_s—half-saturation constant of growth ($\mu g\ P\ l^{-1}$)
Q_{PP}, Q_{SP}—cell quotas of particulate and surplus (P ($\mu g\ P\ mg^{-1}$ C)
$Q_{PP,0}$, $Q_{SP,0}$—maintenance cell quotas of particulate and surplus P ($\mu g\ P\ mg^{-1}$ C)
Q_{PN}, $Q_{PN,0}$—cell quota and maintenance cell quota of particulate N ($\mu g\ N\ mg^{-1}$ C)
k^+, k^-—net rates of population change (day^{-1})
μ/μ'_m—relative growth rate (dimensionless)

Phosphate uptake

k_{gross}, k_{leak}—specific rate constants of gross P uptake and P leakage ($mg\ C^{-1}\ h^{-1}$)
TT—turnover time of orthophosphate in the water (h)
v_{net}, v_{gross}, v_{leak}—specific net, gross and leakage rates of P uptake ($\mu g\ P\ mg^{-1}$ C h^{-1})
L_P—specific conductivity coefficient ($\mu g\ P\ mg^{-1}\ C\ h^{-1}$)
$[P_e]$, $[P_e]_0$, $[P_a]$—external, initial and added orthophosphate concentration ($\mu g\ P\ l^{-1}$)
$[P_e]_T$, $[P'_e]_T$—threshold and apparent threshold concentration ($\mu g\ P\ l^{-1}$)
u_P—specific rate of steady-state net P uptake ($\mu g\ P\ mg^{-1}$ C day^{-1})

Other symbols

*—the variable was normalized to estimated cell carbon
PDI—phosphorus deficiency indicator ($\mu g\ C\ \mu g^{-1}\ P$)
Z_{eu}, Z_m—the euphotic and the mixing depth (m)

References

Ahlgren,I. and Ahlgren,G. (1976) *Analytical Methods for Water Chemistry*. Institute of Limnology, Uppsala University, 80 pp.

Auer,M.T., Kieser,M.S. and Canale,R.P. (1986) Identification of critical nutrient levels through field verification of models for phosphorus and phytoplankton growth. *Can. J. Fish. Aquat. Sci.*, **43**, 379–388.

Bell,R.T., Stensdotter,U., Istvánovics,V., Pierson,D. and Pettersson,K. (1994) Microbial dynamics and nutrient turnover in Lake Erken, in preparation.

Braunwarth,C. and Sommer,U. (1985) Analyses of the *in situ* growth rates of Cryptophyceae by use of the mitotic index technique. *Limnol. Oceanogr.*, **30**, 893–897.

Brekke,O. (1987) Phosphorus limited growth and phosphate uptake of freshwater algae: Chemostat studies of *Rhodomonas lacustris* (Cryptophyceae) and competition studies in a eutrophic lake (in Norwegian). CS Thesis, University of Trondheim, Trondheim, Norway.

Button,D.K. (1985) Kinetics of nutrient-limited transport and microbial growth. *Microbiol. Rev.*, **49**, 270–297.

Currie,D.J. and Kalff,J. (1984) The relative importance of bacterioplankton and phytoplankton in phosphorus uptake in freshwater. *Limnol. Oceanogr.*, **29**, 311–321.

Dokulil,M. (1979) Seasonal pattern of phytoplankton. In Löffler,H. (ed.), *Neusiedlersee: The limnology of a shallow lake in central Europe*. Dr W.Junk, The Hague, pp. 203–231.

Droop,M.R. (1973) Some thoughts on nutrient limitation in algae. *J. Phycol.*, **9**, 264–272.

Falkner,G., Falkner,R. and Schwab,A.J. (1989) Bioenergetic characterization of transient state phosphate uptake by the cyanobacterium *Anacystis nidulans*. *Arch. Microbiol.*, **152**, 353–361.

Falkner,R. and Falkner,R. (1989) Phosphate uptake by eucaryotic algae in cultures and by a mixed phytoplankton population in a lake: Analysis by a force–flow relationship. *Bot. Acta*, **102**, 283–286.

Fitzgerald,C.P. and Nelson,T. (1966) Extractive and enzymatic analyses for limiting and surplus phosphorus in algae. *J. Phycol.*, **2**, 32–37.

Harris,G.P. (1986) *Phytoplankton Ecology*. Chapman and Hall, London, 384 pp.

Istvánovics,V. and Herodek,S. (1995) Estimation of net uptake and leakage rates of orthophosphate from ^{32}P uptake kinetics by a linear force–flow model. *Limnol. Oceanogr.*, in press.

Istvánovics,V., Pettersson,K. and Pierson,D. (1990) Partitioning of phosphate uptake between different size groups of planktonic microorganisms in Lake Erken. *Verh. Int. Ver. Limnol.*, **24**, 231–235.

Istvánovics,V., Pettersson,K., Pierson,D. and Bell,R. (1992) Evaluation of phosphorus deficiency indicators for summer phytoplankton in Lake Erken. *Limnol. Oceanogr.*, **37**, 890–900.

Istvánovics,V., Pettersson,K., Rodrigo,M.A., Pierson,D., Padisák,J. and Colom,W. (1993) *Gloeotrichia echinulata*, a colonial cyanobacterium with a unique phosphorus uptake and life strategy. *J. Plankton Res.*, **15**, 531–552.

Lean,D.R.S. and Nalewajko,C. (1976) Phosphate exchange and organic phosphorus excretion by freshwater algae. *J. Fish. Res. Board Can.*, **33**, 1312–1323.

Lean,D.R.S. and Pick,F.R. (1981) Photosynthetic response of lake plankton to nutrient enrichment: A test for nutrient limitation. *Limnol. Oceanogr.*, **26**, 1001–1019.

Lean,D.R.S and White,E. (1983) Chemical and radiotracer measurements of phosphorus uptake by lake plankton. *Can. J. Fish. Aquat. Sci.*, **40**, 147–155.

Lehman,J.T. and Sandgren,C.D. (1982) Phosphorus dynamics of the prokaryotic nanoplankton in a Michigan lake. *Limnol. Oceanogr.*, **27**, 828–838.

Lund,J.W.G., Kipling,C. and Le Cren,E.D. (1958) The inverted microscope method of estimating algal numbers and the statistical basis of estimations by counting. *Hydrobiologia*, **11**, 143–170.

Menzel,D.H. and Corvin,N. (1965) The measurement of total phosphorus in seawater based on the liberation of organically bound fractions by persulfate oxidation. *Limnol. Oceanogr.*, **10**, 280–282.

Monod,J. (1950) La technique de la culture continue: Theorie et applications. *Ann. Inst. Pasteur Lille*, **79**, 390–410.

Murphy,J. and Riley,J.P. (1962) A modified single solution method for the determination of phosphate in natural waters. *Anal. Chem. Acta*, **27**, 31–36.

Nalewajko,C. and Lean,D.R.S. (1978) Phosphorus kinetics—algal growth relationships in batch cultures. *Mitt. Int. Ver. Limnol.*, **21**, 184–192.

Nauwerck,A. (1963) Die Beziehungen zwischen Zooplankton und Phytoplankton im See Erken. *Symb. Bot. Ups.*, **17/5**, 1–163.

Németh,J. and Vörös,L. (1986) Theory and methodology of algological monitoring in surface waters (in Hungarian). OKTH A/12 6/1, Budapest.

Olsen,Y., Jensen,A., Reinertsen,H. and Rugstad,B. (1983) Comparison of different algal carbon estimates by use of the Droop-model for nutrient limited growth. *J. Plankton Res.*, **5**, 43–51.

Pettersson,K. (1980) Alkaline phosphatase activity and algal surplus phosphorus as phosphorus-deficiency indicators in Lake Erken. *Arch. Hydrobiol.*, **89**, 54–87.

Pettersson,K. (1985) Vattenöversikt Broströmmens vattensystem 1984. Report LIU 1985B:1. Institute of Limnology, Uppsala University, Uppsala, Sweden (in Swedish).

Pettersson,K., Istvánovics,V. and Pierson,D. (1990) Effects of vertical mixing on phytoplankton phosphorus supply during summer in Lake Erken. *Verh. Int. Ver. Limnol.*, **24**, 236–241.

Pettersson,K., Bell,R., Istvánovics,V., Padisák,J. and Pierson,D. (1993) Phosphorus status of size-fractionated seston in Lake Erken. *Verh. Int. Ver. Limnol.*, **25**, 137–143.

Pierson,D.C. (1990) Effects of vertical mixing on phytoplankton photosynthesis and phosphorus deficiency. PhD Thesis. Institute of Limnology, Uppsala University, Uppsala, Sweden.

Pierson,D.C., Pettersson,K. and Istvánovics,V. (1992) Temporal changes in biomass specific photosynthesis during the summer: regulation by environmental factors and the importance of phytoplankton succession. *Hydrobiologia*, **243/244**, 119–135.

Reynolds,C.S. (1988) Functional morphology and the adaptive strategies of freshwater phytoplankton. In Sandgren,C.D. (ed.), *Growth and Reproductive Strategies of Freshwater Phytoplankton*. Cambridge University Press, Cambridge, pp. 388–434.

Reynolds,C.S. (1989) Physical determinants of phytoplankton succession. In Sommer,U. (ed.), *Plankton Ecology*. Springer-Verlag, Berlin, pp. 9–57.

Reynolds,C.S., Wiseman,S.W. and Clarke,M.J.O. (1984) Growth- and loss-rate responses of phytoplankton to intermittent artificial mixing and their potential application to the control of planktonic algal biomass. *J. Appl. Ecol.*, **21**, 11–39.

Rhee,G.-Y. (1973) A continuous culture study of phosphate uptake, growth rate, and polyphosphate in *Scenedesmus* sp. *J. Phycol.*, **9**, 495–506.
Rigler,F.H. (1966) Radiobiological analysis of inorganic phosphorus in lake water. *Verh. Int. Ver. Limnol.*, **16**, 466–470.
Rocha,O. and Duncan,A. (1985) The relationship between cell carbon and cell volume in freshwater algal species used in zooplankton studies. *J. Plankton Res.*, **7**, 279–294.
Sakshaug,E., Andersen,K., Myklestad,S. and Olsen,Y. (1983) Nutrient status of phytoplankton communities in Norwegian waters (marine, brackish and fresh) as revealed by their chemical composition. *J. Plankton Res.*, **5**, 175–196.
Smith,R.E.H. and Kalff,J. (1983) Competition for phosphorus among co-occurring freshwater phytoplankton. *Limnol. Oceanogr.*, **28**, 448–464.
Sommer,U. (1981) The role of r- and K-selection in the succession of phytoplankton in Lake Constance. *Acta Ecol. Ecol. Gener.*, **2**, 327–342.
Sommer,U. (1984) The paradox of the plankton: Fluctuations of phosphorus availability maintain diversity of phytoplankton in flow-through cultures. *Limnol. Oceanogr.*, **29**, 633–636.
Sommer,U. (1986) The periodicity of phytoplankton in Lake Constance (Bodensee) in comparison to other deep lakes in central Europe. *Hydrobiologia*, **138**, 1–7.
Sommer,U. (1989a) The role of competition for resources in phytoplankton succession. In Sommer,U. (ed.), *Plankton Ecology*. Springer-Verlag, Berlin, pp. 57–107.
Sommer,U. (1989b) Nutrient status and nutrient competition of phytoplankton in a shallow, hypertrophic lake. *Limnol. Oceanogr.*, **34**, 1162–1173.
Strickland,J.D.H. and Parsons,T.R. (1972) *A Practical Handbook of Seawater Analysis. Bull. 167*, Fisheries Research Board, Ottawa, Canada.
Tilman,D. (1977) Resource competition between planktonic algae: an experimental and theoretical approach. *Ecology*, **58**, 338–348.
Tilman,D. and Kilham,S.S. (1976) Phosphate and silicate growth and uptake kinetics of the diatoms *Asterionella formosa* and *Cyclotella meneghiniana* in batch and semicontinuous culture. *J. Phycol.*, **12**, 375–383.
Tilman,D., Kilham,S.S. and Kilham,P. (1982) Phytoplankton community ecology: the role of limiting nutrients. *Annu. Rev. Ecol. Syst.*, **13**, 349–372.
Vadstein,O. and Olsen,Y. (1989) Chemical composition and phosphate uptake kinetics of limnetic bacterial communities cultured in chemostats under phosphorus limitation. *Limnol. Oceanogr.*, **34**, 939–946.
Vadstein,O., Jensen,A., Olsen,Y. and Reinertsen,H. (1988) Growth and phosphorus status of limnetic phytoplankton and bacteria. *Limnol. Oceanogr.*, **33**, 489–503.
Vörös,L. and Padisák,J. (1991) Phytoplankton biomass and chlorophyll-*a* in some shallow lakes in central Europe, *Hydrobiologia*, **215**, 111–119.

Received on January 2, 1994; accepted on May 4, 1994